Japanese Journal of Applied Physics **53**, 07KF25 (2014) **REGULAR PAPER**
http://dx.doi.org/10.7567/JJAP.53.07KF25

Ultrasonic visualization of propagation of myocardial vibration driven by electrical excitation of myocardium of rat in ex vivo experiment

Yuta Fujita[1], Hideaki Tagashira[2], Hideyuki Hasegawa[1,3], Kohji Fukunaga[2], and Hiroshi Kanai[3,1*]

[1]*Graduate School of Biomedical Engineering, Tohoku University, Sendai 980-8579, Japan*
[2]*Graduate School of Pharmaceutical Sciences, Tohoku University, Sendai 980-0845, Japan*
[3]*Graduate School of Engineering, Tohoku University, Sendai 980-8579, Japan*
E-mail: kanai@ecei.tohoku.ac.jp

Received November 29, 2013; accepted April 21, 2014; published online June 26, 2014

For the realization of noninvasive and regional myocardial tissue characterization, in the present study, we attempted to elucidate the characteristics of the myocardial response to electrical excitation and its propagation by an ex vivo experiment using a rat left ventricular wall. To visualize such a propagation phenomenon, whose speed is up to several m/s, high-frame-rate ultrasound was used to measure the myocardial vibrations driven by electrical excitation at 72 points along the heart wall with 200 μm intervals at a frame rate of 3472 Hz. The propagation of myocardial vibration was visualized by estimating the delay time between vibration waveforms measured in the reference ultrasonic beam and each ultrasonic beam using the cross-correlation function between the vibration waveforms. From the estimated delay time, we visualized the propagation of myocardial vibration caused by electrical excitation. The propagation speed was estimated to be 2.5 m/s in the entire excised myocardium. It was also estimated to be 1.8 m/s in the middle of the heart wall and 2.2 m/s at the internal and external surfaces of the left-ventricular wall. The results showed that the myocardial vibration driven by electrical excitation could be measured with high-frame-rate ultrasound.
© 2014 The Japan Society of Applied Physics

1. Introduction

About 7.3 million people in the world and 20 thousand people in Japan die of heart diseases in a year.[1,2] Serious heart diseases require a long-term advanced care and enormous costs for treatment. For example, the cost for health care in Japan was 742 million yen in 2011.[3] Therefore, the selection of an appropriate treatment and the prevention of the onset of such diseases are essential. To that end, there is a need for developing accurate diagnostic methods that can be applied repeatedly to monitor the condition of a patient.

Electrocardiography,[4] chest X-ray, computed tomography (CT),[5] magnetic resonance imaging (MRI),[6,7] and ultrasound[8] are commonly used for the diagnosis of heart diseases. Electrocardiography is an invaluable clinical tool for the diagnosis of cardiac failure. Chest X-ray can be used to diagnose pathological conditions, but further diagnosis, such as an invasive catheterization, must be performed if the required information cannot be obtained. CT and MRI enable morphological diagnosis from three-dimensional images and the evaluation of coronary artery stenosis with contrast agents. Although conventional ultrasonography enables morphological diagnosis, it is also used for the evaluation of heart wall motion[9–11] and myocardial tissue characterization.[12,13] It is very useful because abnormal wall motion occurs frequently in cases of heart diseases. Also, myocardial tissue changes due to heart diseases. However, a new method is necessary for the identification of the diseased region, such as the regional infarcted area in the heart wall, for the accurate diagnosis of heart diseases.

Our study group previously examined the rapid response of the excised myocardium of a rat driven by electrical excitation (change in thickness of 30 μm and vibration velocity of 0.5 mm/s).[14] From our findings, we measured the propagation of vibration in the interventricular septum at about 10,000 points caused by the conduction of the electrical excitation[15] in vivo. Furthermore, we showed possibilities of the ultrasonic measurement of the propagation of myocardial contraction in response to the electrical excitation in vivo.[16]

In our previous ex vivo experiments using an excised myocardium of a rat, the propagation of myocardial vibration driven by electrical excitation was not identified because the myocardial vibration was measured at only one point on the myocardial tissue using laser velocimetry. Therefore, the causality among the electrical excitation, myocardial vibration, and its propagation is still unclear. Therefore, in the present study, we measured the myocardial contraction response driven by electrical excitation ex vivo at high temporal and spatial resolutions using ultrasound. Electrical excitation propagates at a velocity of several m/s.[17–20] Therefore, in the present study, myocardial vibrations were measured at a high temporal resolution of 3472 Hz with high-frame-rate ultrasound.

2. Materials and methods

2.1 Experimental setup

Figure 1 shows a schematic diagram of the experimental system used to measure the propagation of myocardial vibration driven by electrical excitation. The specimen used was the left ventricular wall excised from the heart of a Sprague-Dawley rat (11 weeks old, 368.1 g). The size of the myocardium was $5.1 \times 15.4\,\mathrm{mm}^2$. The myocardium was fixed by hooks attached to an XY stage and a force transducer (Fig. 2). The force transducer was employed to measure the tension $T(t)$ along the longitudinal axis of the myocardium generated by myocardial contraction. The myocardium was stimulated from the apical side by an electrical stimulator as in the propagation of the electrical excitation in vivo. In addition, the ventricular cavity side of the myocardium was placed near the ultrasonic probe. The water tank was filled with Krebs-Henseleit solution, which was warmed at 37 °C, and 95% O_2 gas was richly melted into the solution. The size of the tank was $100 \times 100 \times 100\,\mathrm{mm}^3$. The absorbing material was placed at the bottom of the water tank in order to reduce the effect of reflected ultrasonic waves. The myocardium was electrically stimulated by a rectangular

© 2014 The Japan Society of Applied Physics

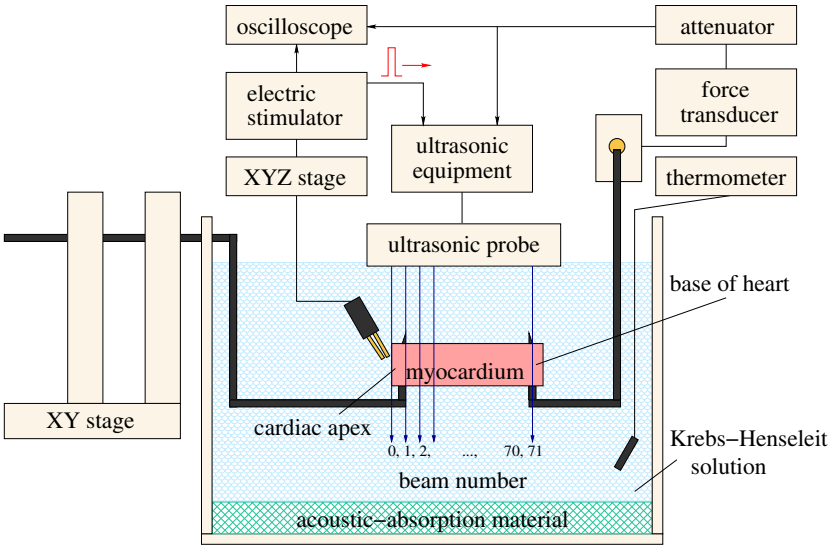

Fig. 1. (Color online) Experimental setup for measuring the vibration of the myocardium extracted from the excised rat heart.

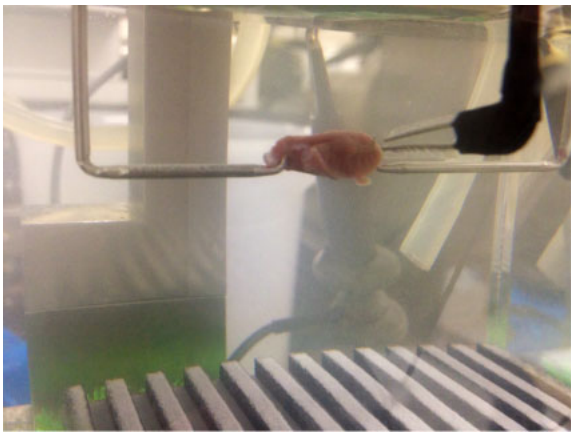

Fig. 2. (Color online) Myocardium fixed by two hooks.

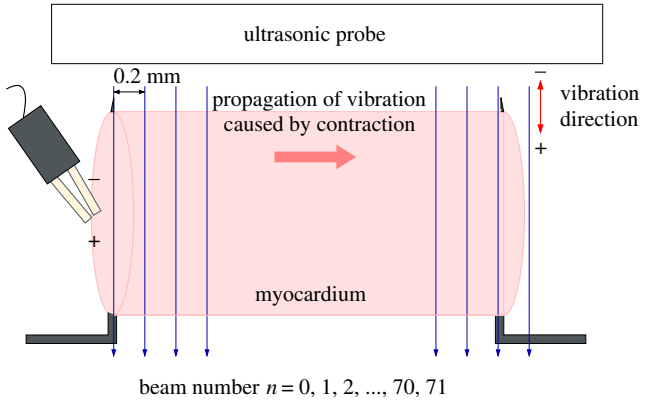

Fig. 3. (Color online) Illustration of measurement of minute vibration velocity waveforms. Spacings of ultrasonic RF data were 0.2 mm and 20 μm in the axial and lateral directions, respectively.

pulse $e(t)$ at a repetition frequency of 2 Hz at 4 V. Platinum electrodes were attached to an XYZ stage for the adjustment of the geometry. By adjusting the voltage and the distance of the edge of the myocardium from the electrodes, only a very small part of the myocardium at the edge could be activated by electrical excitation, and the subsequent propagation of the myocardial contraction to the other side of the myocardium could be observed. Electrodes were coated with plastic paste other than their tips in order to prevent the formation of extra electric fields in the solution. The distance between the myocardium and the electrodes was about 1.0 mm. The pulse waveform was also input to the ultrasound system for data acquisition. The acquisition of ultrasonic data was triggered by electrical stimulation.

2.2 Acquisition of ultrasonic data

The vibration velocity $v(t)$ caused by myocardial contraction in response to electrical excitation was measured by ultrasound. Figure 3 illustrates the propagation of the myocardial contraction response.

To measure myocardial vibrations at a high temporal resolution, parallel beam forming (PBF)[21,22] was performed with ultrasonic diagnostic equipment (Hitachi-Aloka ProSound α-10) equipped with a 10 MHz linear array probe. In this method, the number of transmissions was reduced using plane waves in transmission and creating multiple focused receiving beams per transmission. In the present study, the number of transmissions was 3, and 72 receiving beams were obtained by 3 transmissions. As a result, a high frame rate ($1/\Delta T$; ΔT: frame interval) of 3472 Hz was realized. The sampling frequency of the beamformed RF signal was 40 MHz. Figure 4 shows a B-mode image of the myocardium.

Vibration velocities were estimated along 72 beams (beam number $M = 0, 1, \ldots, 71$) with intervals of 0.2 mm. Along each beam, vibration velocities were estimated at intervals of 20 μm in the axial direction. In the present study, the minute vibration velocity $v(t)$ caused by myocardial contraction was measured by the *phased-tracking method*.[23] The *phased-tracking method* has been used for determining cardiovascular dynamics[24,25] and also for obtaining morphological information.[26,27] The average velocity $v(t + \Delta T/2)$ of an object at the frame interval ΔT is accurately estimated using the phase shift between the received ultrasonic pulses as

© 2014 The Japan Society of Applied Physics

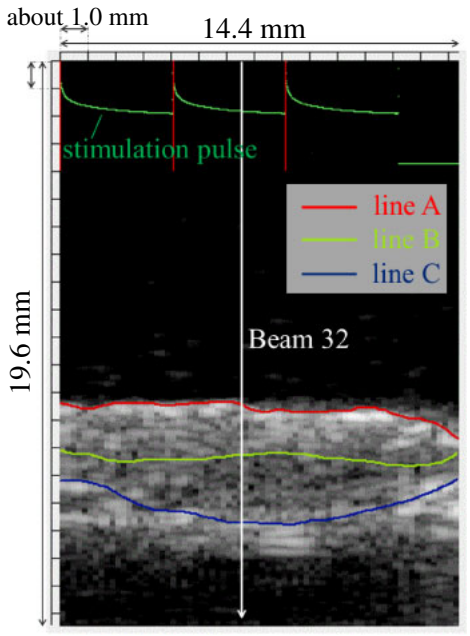

Fig. 4. (Color online) Cross-sectional view of the myocardium and manually assigned lines for analysis.

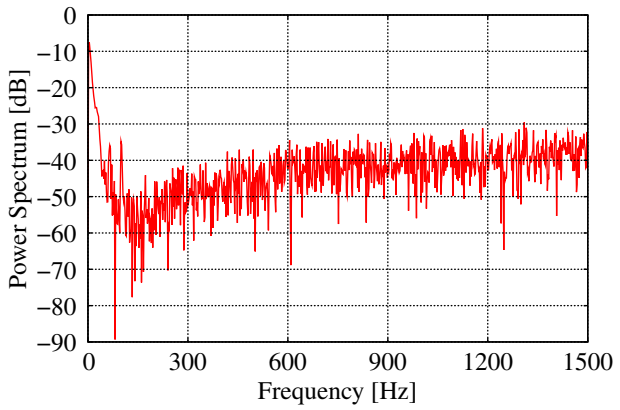

Fig. 5. (Color online) Frequency components of the vibration velocity waveform by myocardium contraction.

$$v\left(t+\frac{\Delta T}{2}\right)=c_0\frac{\Delta\theta(x;t)}{4\pi f_0\Delta T}, \tag{1}$$

where c_0 is the velocity of ultrasound, f_0 is the center frequency, and $\Delta\theta(x;t)$ is the phase shift of the received ultrasound signal during ΔT.

A low-pass filter with a cutoff frequency of 700 Hz was applied to the estimated vibration velocity $v(t)$ to reduce the high-frequency noise. The cutoff frequency of 700 Hz was selected so as not to remove velocity components due to myocardial contraction (from 0 to 150 Hz)[23] (Fig. 5). Also, a low-pass filter with a cutoff frequency of about 35 Hz was applied to the measured tension $T(t)$ to reduce electrical noise. Furthermore, for the confirmation of myocardial contraction, the change in the thickness of the myocardium was also estimated by the temporal integration of the difference between velocities at the near and far surfaces of the myocardium.[28]

2.3 Visualization of distribution of propagation time delays of vibrations

In the present study, the propagation of myocardial vibration was visualized by estimating its delay time. The propagation delay time was defined as the delay time of the vibration velocity $v_{j,i}(n)$ measured in each (i-th) ultrasonic beam from that measured in the reference beam. The distributions of propagation delays were obtained along three manually assigned lines (lines A, B, and C in Fig. 4) at different depths j ($j=0$, 1, and 2). To consider the difference in fiber direction between the inside and surface of the myocardium, propagation speeds were measured on 3 lines. Lines A and C were selected to measure the propagation speed at the surface of the myocardium, and line B was selected to measure the propagation speed inside the myocardium.

The delay time was estimated using the cross-correlation function[29] between the vibration velocities $v_{j,\mathrm{Ref}}(n)$ and $v_{j,i}(n)$ (n: frame number) in the reference and each beams. The cross-correlation function $r_{j,i}(m)$ is expressed as

$$r_{j,i}(m)=\frac{1}{\sigma_{j,\mathrm{Ref}}\sigma_{j,i}N}\sum_{n=0}^{N-1}(v_{j,\mathrm{Ref}}(n)-\bar{v}_{j,\mathrm{Ref}})\times(v_{j,i}(n+m)-\bar{v}_{j,i}), \tag{2}$$

where $\sigma_{j,\mathrm{Ref}}$ and $\sigma_{j,i}$ are the standard deviations of $v_{j,\mathrm{Ref}}(n)$ and $v_{j,i}(n)$ for N frames, respectively. Moreover, $\bar{v}_{j,\mathrm{Ref}}$ and $\bar{v}_{j,i}$ are averages of $v_{j,\mathrm{Ref}}(n)$ and $v_{j,i}(n)$ for N frames, respectively. The delay time $\tau_{j,i}$ values were determined from the lag $m_{\max}$, which maximizes the cross-correlation function, as $m_{\max}\cdot\Delta T$.

To estimate the propagation speed of myocardial vibration, the estimated delay time $\tau_{j,i}$ values were plotted as a function of beam position $i\cdot\Delta x$ (Δx: interval of beams). Then, the linear regression line was determined by the least-squares method.[30] The propagation speed c_s was estimated by the inverse of the slope of the determined regression line. By repeating the same procedure for other depths j, propagation speeds c_s at different depths j were estimated.

3. In vitro experimental results

Figure 4 shows a B-mode image of the myocardium measured in the present study. There are electrodes near the 0th ultrasonic beam that corresponds to the left edge of the B-mode. Vibration velocities $v(t)$ were estimated along lines A–C.

Figure 6 shows the measured myocardial contraction response driven by electrical excitation. Figure 6(b) shows the vibration velocities $v_{0,32}(t)$; $v_{2,32}(t)$, and the amplitude of $v_{2,32}(t)$ is smaller than that of $v_{0,32}(t)$. The myocardial contraction was triggered by the electrical stimulation signal $e(t)$ shown in Fig. 6(a). The change in the thickness of the myocardium $\hat{h}(t)$ was obtained as shown in Fig. 6(c) by the temporal integration of the difference between $v_{0,32}(t)$ and $v_{2,32}(t)$. The tension $T(t)$ measured by the force transducer was also obtained as shown in Fig. 6(d). Unfortunately, the generated force was very small, and the signal-to-noise ratio of the tension waveform was very low. However, it can be observed that the tension was generated by electrical stimulation. These results show that myocardial contraction was caused by electrical excitation.

Figure 7 shows the vibration velocities v_0–v_{71} measured in each line. Around the 0th and 71st beams, amplitudes of

© 2014 The Japan Society of Applied Physics

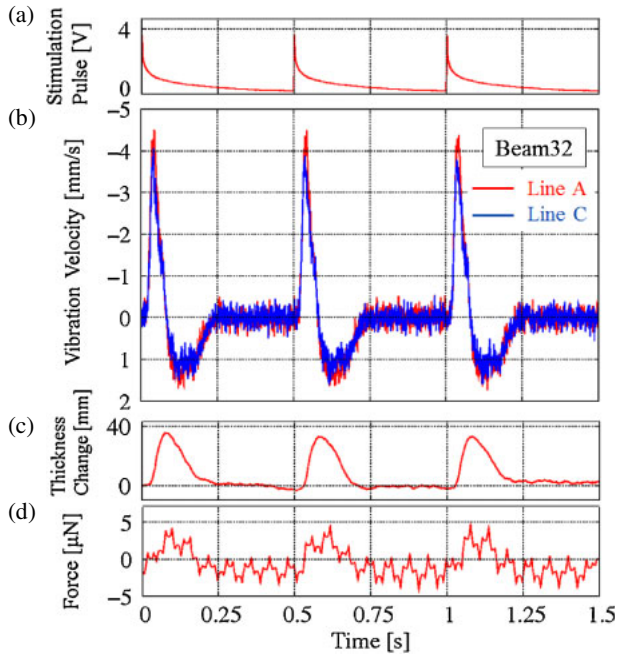

Fig. 6. (Color online) (a) Electrical stimulation pulses $e(t)$ at a repetition frequency of 2 Hz. (b) Measured vibration velocities $v_{0,32}(t)$ and $v_{1,32}(t)$ in lines A and C in Fig. 4, respectively. (c) Change in thickness $\hat{h}(t)$ of the myocardium estimated from (b). (d) Output $T(t)$ of the force transducer.

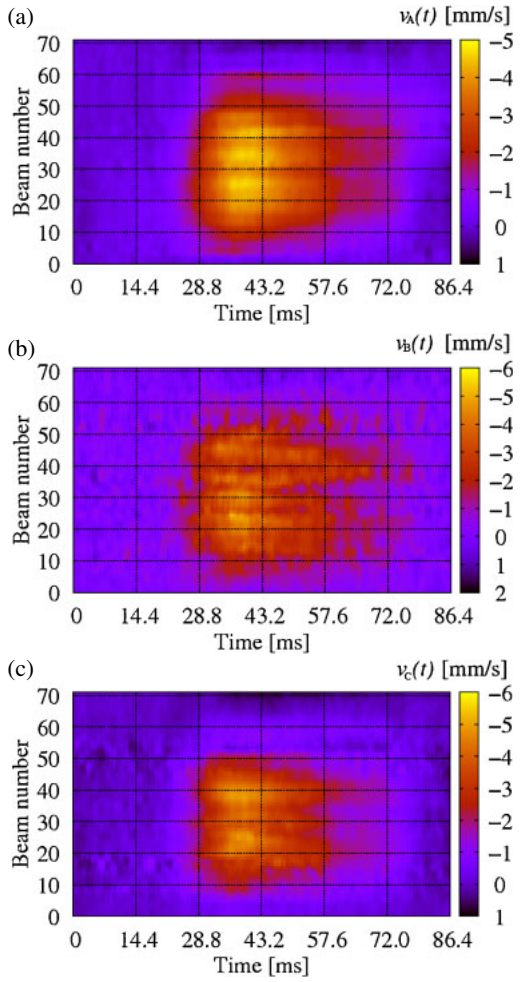

Fig. 7. (Color online) Visualization of vibration velocities v_0–v_{71} along each line.

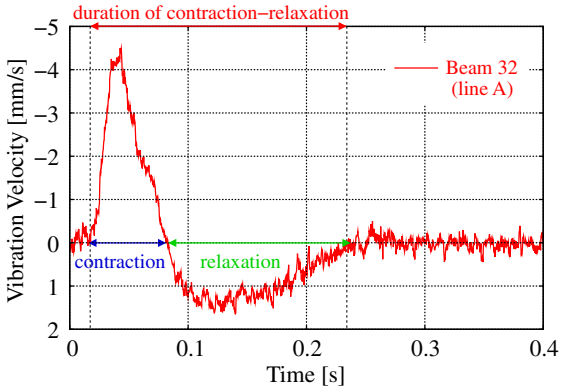

Fig. 8. (Color online) Vibration velocity $v_{32}(t)$ in line A in Fig. 4 and illustration of durations of contraction–relaxation, contraction, and relaxation.

vibration velocities are smaller than those around the central beam because there were hooks near the 0th and 71st beams. From the waveforms of the measured vibration velocities, the durations of contraction and subsequent relaxation, contraction only, and relaxation only were manually estimated as illustrated in Fig. 8. The estimated durations were obtained as the averages for three contraction–relaxation cycles with respect to line A in each beam (from 30th to 40th beams). The vibration velocities $v_{30}(t)$–$v_{40}(t)$ were analyzed because the fixation by the hooks hardly had any effect. The average durations of contraction–relaxation, contraction, and relaxation were estimated to be 242, 74, and 168 ms, respectively.

Figures 9(a)–9(c) show the cross-sectional B-mode image of the myocardium, the delay time distribution of myocardial vibrations, and the average delay time plotted as a function of distance from the reference point, respectively. The delay time of the myocardial vibration at each spatial point was calculated as the delay time from the myocardial vibration at the reference point (4th ultrasonic beam position). The reference point was closer to the stimulation electrode, and the delay time increased when the distance from the reference point (beam 4) increased, as shown in Fig. 9(c). By estimating the regression line using the least-squares method, the propagation speed c_s was estimated to be 2.5 m/s.

For a more detailed analysis of propagation of contraction, we examined the regional propagation of contraction inside and at the surface of the myocardium. Figure 10 shows the delay time distributions of vibration velocities obtained along lines A, B, and C. Vibration velocities were estimated at additional spatial points in the region with a width of 300 μm in depth from each line. In Fig. 10, the reference beam was the 4th beam (beam number $m = 4$). As can be seen in Fig. 10, although slight variations exist, the estimated delay times were similar in the 300 μm regions from the respective lines (A, B, and C) in the same ultrasonic beam. Therefore, the delay time at each ultrasonic beam was obtained by averaging the delay times in the 300 μm region along the corresponding beam around the line of interest (A or B or C) for a stable estimation of the propagation speed of the electrical excitation. Figure 11 shows the average delay times plotted as a function of the distance from the reference beam ($m = 4$) obtained with respect to lines A, B, and C.

© 2014 The Japan Society of Applied Physics

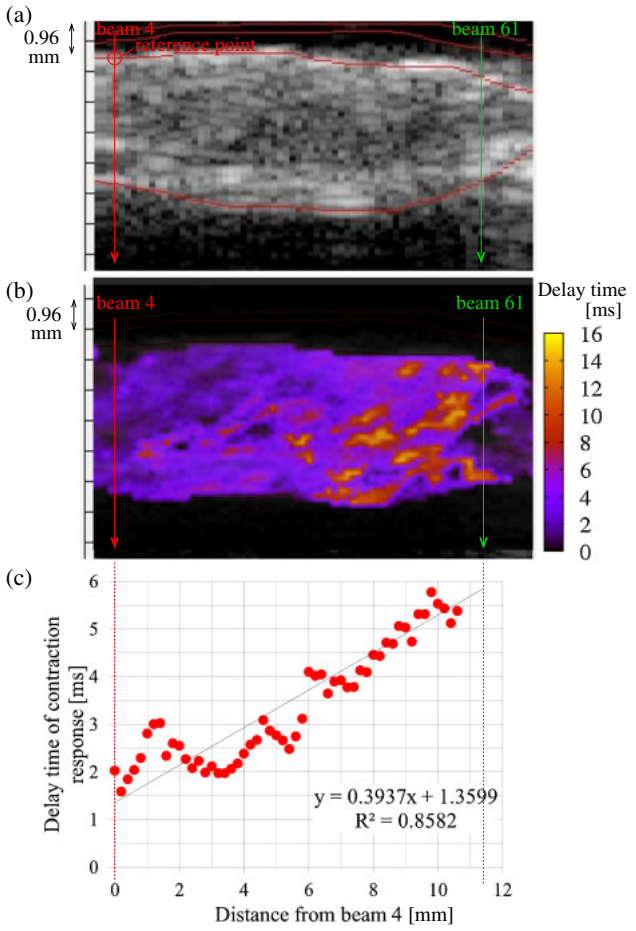

Fig. 9. (Color online) (a) Cross-sectional view of the myocardium. (b) Delay time distribution of myocardial vibrations. (c) Average delay times plotted as a function of distance from the reference point.

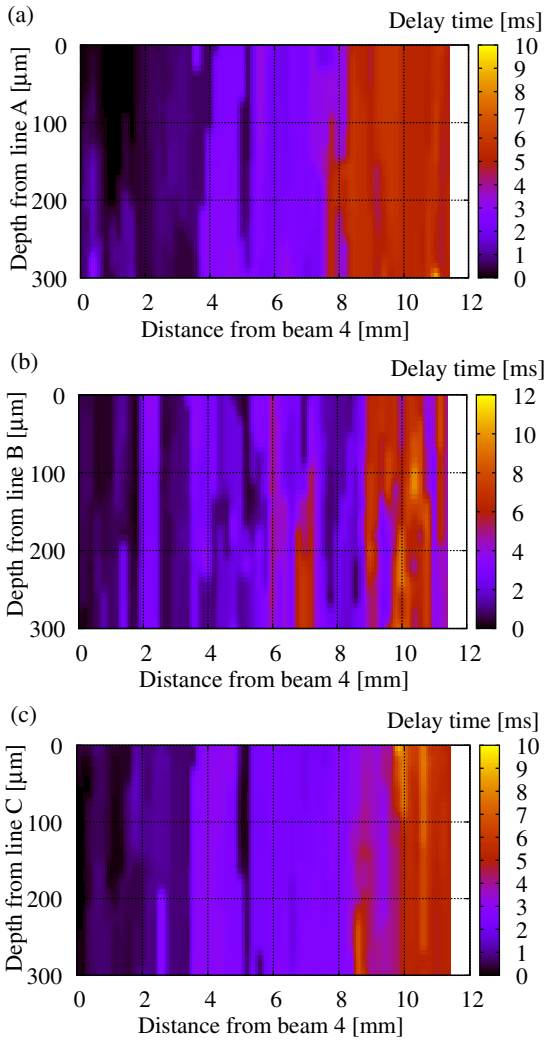

Fig. 10. (Color online) Delay time distributions of myocardial vibrations in the regions of 300 μm from lines A (a), B (b), and C (c).

By estimating the regression line using the least-squares method, the propagation speed c_s was estimated to be 1.8 m/s (line A), 2.2 m/s (line B), and 2.2 m/s (line C).

Furthermore, the time of the beginning of contraction t_c from the electrical stimulation was also estimated using the estimated propagation speed of the electrical excitation. The propagation velocity c_s along line A was used because the correlation between the measured delay time and the regression line was highest ($R^2 = 0.8735$). To obtain the time of the beginning of contraction t_c, the time at the rising edge of the vibration velocity measured in the 4th beam was manually identified to be 19.6 ms. Then, the time required for the electrical excitation to propagate from the edge of the myocardium to the 4th beam was estimated to be 0.87 ms by dividing the distance (3.4 mm) from the edge of the myocardium to the 4th beam by the propagation velocity c_s of 2.5 m/s. Finally, the time of the beginning of contraction t_c was estimated to be (19.6 ms) − (1.34 ms) = 18.3 ms by assuming that the propagation delay of the electric field to propagate from the electrode to the edge of the myocardium was negligible (propagation speed was that of light in water).

4. Discussion

In the present ex vivo experiment, after setting the voltage of the electrical stimulation pulse, the electrodes were put closer to the myocardium. This movement of the electrodes was stopped when the myocardium just began to contract. By this procedure, only the edge of the myocardium was stimulated by the electrical stimulation pulse, and we could avoid the stimulation of the entire myocardium at the same time. However, the electrical voltage at each part of the myocardium could not be measured in the present study, and the distribution of the electrical field in the myocardium is expected to be measured in our future work.

In Fig. 6, the input signal for electrical stimulation $e(t)$ was a rectangular pulse. However, the actual measured waveform became a gradually descending waveform because Krebs–Henseleit solution contained a large amount of electrolyte. There is no effect on contraction because this phenomenon also occurs in the ventricular muscle in vivo.[31] In addition, the measured tension $T(t)$ was affected by electrical noise. We need to modify the experimental system to measure the tension waveform with much better signal-to-noise ratio. In our previous study, we measured the contractional characteristics using papillary muscle.[14] The tension $T(t)$ measured previously was 0.5 mN (100 times larger) and the previously measured change in thickness $\hat{h}(t)$ was similar to that measured in the present study. This is because electrodes were placed parallel against the papillary muscle and the

© 2014 The Japan Society of Applied Physics

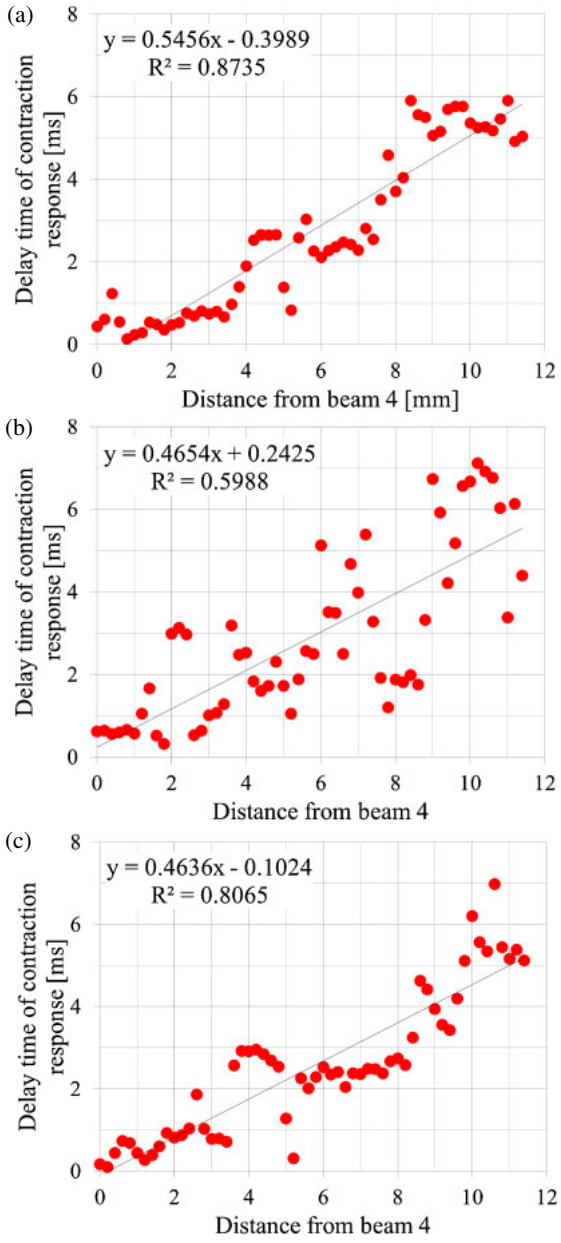

Fig. 11. (Color online) Average delay time plotted as a function of distance from the reference beam (4th beam). The regression lines were determined by the least squares-method. (a) Line A. (b) Line B. (c) Line C.

papillary muscle was stimulated by an electrical pulse with an amplitude that was 2.5 times larger than that in the present study. On the other hand, the times of the beginning of contraction t_c after the electrical stimulations were very similar (about 19.0 ms) in the two studies.

In Fig. 9(b), the points with low brightnesses, whose acoustic impedance is supposed to be low, show slow contraction responses. Therefore, elastic moduli of these points would be small, and small elastic moduli might lead to slow contraction responses.

In Fig. 11, the correlation coefficients R^2 in (b) and (c) ($R^2 = 0.3$ and 0.7, respectively) were lower than that in (a) ($R^2 = 0.8$). Along line B, myocardial vibration velocities were not obtained with good signal-to-noise ratios because the amplitudes of ultrasonic echoes from the inside of the myocardium were small. Although the depth of line C is larger than that of line A, ultrasonic echoes could be obtained with a better signal-to-noise ratio in line C than in line B. However, there are distinct peaks in Fig. 11(c) at distances from the 4th beam of 2, 4, and 6 mm. There are coronary arteries on the external surface of the myocardium (corresponding to line C), and coronary arteries might affect the propagation phenomenon.

It is known that the conduction speed of the electrically excited wave along the human ventricular muscle is about 0.3–1.0 m/s.[32] In the present study, however, the propagation speed of myocardial vibration c_s driven by electrical excitation was estimated to be 1.8–2.5 m/s, corresponding to the conduction speed in Purkinje fibers. The specific resistance of a Purkinje fiber is smaller than that of a ventricular muscle in a mammalian heart.[33,34] Therefore, the electrical excitation might not only propagate through a ventricular muscle but also through a Purkinje fiber. Such a propagation speed of 4 m/s was also found in the propagation from the base side of the intraventricular septum (IVS) to the apical side in the previous study.[15,32]

The beginning of contraction t_c was delayed from the electrical stimulation pulse by 18.3 ms. To generate the mechanical response (myocardium contraction), Na^+ and Ca^{2+} were introduced into cells by the opening of Na^+ and Ca^{2+} channels by action potential induced by electrical stimulation. This phenomenon leads to the slipping movement of myosin filaments, resulting in the deformation of myofibrils as a trigger of Ca^{2+} inflow. The delay time of 18.3 ms was considered to be caused by the above response to the electrical stimulation.[35,36]

5. Conclusions

In the present study, we performed the ex vivo measurement of the characteristics of the myocardial response to the electrical excitation and the propagation of myocardial vibration in an excised left ventricular myocardium of a rat with high-frame-rate ultrasound. Results indicate that the contractional response occurred about 18.3 ms after the electrical stimulation, followed by a change in thickness, and that a tension of about 5 μN occurred 10.0 ms later. The vibration velocity of the myocardium was estimated to be about 4 mm/s during contraction and about 2 mm/s during relaxation. Durations of contraction–relaxation, contraction only, and relaxation only were also estimated to be 242, 74, and 168 ms, respectively. Furthermore, we visualized the propagation of myocardial vibration, and the propagation speed c_s was estimated to be 1.8–2.5 m/s. From these results, we showed that the propagation of the myocardial contraction response driven by electrical excitation can be measured with ultrasound, and that the visualization of the propagation of myocardial contraction can be useful for the tissue characterization of the regional heart muscle.

1) S. Mendis, P. Puska, and B. Norrving, *Global Atlas on Cardiovascular Disease Prevention and Control* (World Health Organization, Geneva, 2011) p. 3.
2) Ministry of Health, Labour and Welfare, Report of Vital Statistics in 2012, p. 11.
3) Ministry of Health, Labour and Welfare, Overview of National Health Expenditure in 2012 [in Japanese]. [http://www.mhlw.go.jp/toukei/saikin/hw/k-iryohi/10/dl/toukei.pdf] (2013.11.13).

© 2014 The Japan Society of Applied Physics

4) C. Ramanathan, R. N. Ghanem, P. Jia, K. Ryu, and Y. Rudy, Nat. Med. **10**, 422 (2004).
5) L. T. Mahoney, W. Smith, M. P. Noel, M. Florentine, D. J. Skorton, and S. M. Collins, Invest. Radiol. **22**, 451 (1987).
6) L. Axel and L. Dougherty, Radiology **171**, 841 (1989).
7) M. B. Buchalter, J. L. Weiss, W. J. Rogers, E. A. Zerhouni, M. L. Weisfeldt, R. Beyar, and E. P. Shapiro, Circulation **81**, 1236 (1990).
8) K. Hamaoka, S. Ishikawa, T. Itoi, S. Echigo, H. Sumi, H. Kurosawa, S. Sano, M. Nagashima, T. Nakanishi, T. Yagihara, S. Yasui, T. Yamagishi, and M. Yamagishi, Circ. J. **73**, 1115 (2009) [in Japanese].
9) Y.-F. Cheung, Nat. Rev. Cardiol. **9**, 644 (2012).
10) Y. Honjo, H. Hasegawa, and H. Kanai, Jpn. J. Appl. Phys. **51**, 07GF06 (2012).
11) G. R. Sutherland, G. D. Salvo, P. Claus, J. D'hooge, and B. Bijnens, J. Am. Soc. Echocardiogr. **17**, 788 (2004).
12) J. G. Miller, J. E. Perez, and B. E. Sobel, Prog. Cardiovasc. Dis. **28**, 85 (1985).
13) H. Shida, H. Hasegawa, and H. Kanai, Jpn. J. Appl. Phys. **51**, 07GF05 (2012).
14) H. Kanai, S. Katsumata, H. Honda, and Y. Koiwa, Acoust. Sci. Technol. **24**, 17 (2003).
15) H. Kanai, Ultrasound Med. Biol. **35**, 936 (2009).
16) H. Kanai and M. Tanaka, Jpn. J. Appl. Phys. **50**, 07HA01 (2011).
17) D. Durrer, R. T. van Dam, G. E. Freud, M. J. Janse, F. L. Meuler, and R. C. Arzbaecher, Circulation **41**, 899 (1970).
18) A. M. Katz, *Physiology of the Heart* (Lippincott Williams & Wilkins, Philadelphia, PA, 2001) 3rd ed., p. 518.
19) B. Mitrea, B. Caldwell, and A. Pertsov, Biomed. Opt. Express **2**, 620 (2011).
20) A. Scher, A. Young, A. Malmghen, and R. Pation, Circ. Res. **1**, 539 (1953).
21) H. Hasegawa and H. Kanai, IEEE Trans. Ultrason. Ferroelectr. Freq. Control **55**, 2626 (2008).
22) H. Hasegawa, K. Hongo, and H. Kanai, J. Med. Ultrason. **40**, 91 (2013).
23) H. Kanai, M. Sato, Y. Koiwa, and N. Chubachi, IEEE Trans. Ultrason. Ferroelectr. Freq. Control **43**, 791 (1996).
24) K. Ikeshita, H. Hasegawa, and H. Kanai, Jpn. J. Appl. Phys. **51**, 07GF14 (2012).
25) H. Yoshiara, H. Hasegawa, H. Kanai, and M. Tanaka, Jpn. J. Appl. Phys. **46**, 4889 (2007).
26) H. Takahashi, H. Hasegawa, and H. Kanai, Jpn. J. Appl. Phys. **52**, 07HF17 (2013).
27) K. Kitamura, H. Hasegawa, and H. Kanai, Jpn. J. Appl. Phys. **51**, 07GF08 (2012).
28) H. Kanai, H. Hasegawa, N. Chubachi, Y. Koiwa, and M. Tanaka, IEEE Trans. Ultrason. Ferroelectr. Freq. Control **44**, 752 (1997).
29) K. Kido, *Digitaru Shingoshori Nyumon* (Maruzen, Tokyo, 1985) p. 51 [in Japanese].
30) H. Kanai, *Oto Shindo no Supekutoru Kaiseki* (Coronasha, Tokyo, 1992) p. 36 [in Japanese].
31) M. R. Franz, K. Bargheer, W. Rafflenbeul, A. Haverich, and P. R. Lichtlen, Circulation **75**, 379 (1987).
32) D. M. Bers, *Excitation-Contraction Coupling and Cardiac Contractele Force* (Kluwer Academic, Boston, MA, 2001) p. 64.
33) S. Weidmann, J. Physiol. **118**, 348 (1952).
34) S. Weidmann, J. Physiol. **210**, 1041 (1970).
35) S. Sakiyama, *Shin Kino* (Chugai Igakusha, Tokyo, 1990) 2nd ed., p. 21 [in Japanese].
36) J. M. Nerbonne and R. S. Kass, Physiol. Rev. **85**, 1205 (2005).

© 2014 The Japan Society of Applied Physics